Immunobiotic bacteria attenuate fibrosis in Non-alcoholic steatohepatitis mice model: molecular insights and therapeutic potential of immunobiotics for the gut-liver axis

Paulraj Kanmani
University of Illinois
Julio Villena
Reference Centre for Lactobacilli (CERELA-CONICET)
Soo-kyoung Lim
Dongguk University
Eun-Ji Song
Korea Food Research Institute
Young-Do Nam
Korea Food Research Institute
Hojun Kim (kimklar@dongguk.ac.kr)
Dongguk University

Research Article

Keywords: Non-alcoholic steatohepatitis, Liver fibrosis, Immunobiotics, Gut microbiota, Immunoregulation, Amelioration

Posted Date: May 17th, 2022

DOI: https://doi.org/10.21203/rs.3.rs-1644742/v1

Abstract

Background

Non-alcoholic steatohepatitis (NASH) is a leading cause of chronic liver disease worldwide that can progress to liver fibrosis (LF). Probiotics have beneficial roles in reducing intestinal inflammation and gut-associated diseases, but their effects and mechanisms beyond the gut in attenuating the progression of LF are remains unclear.

Results

We used a diet-induced NASH/LF mouse model to examine the therapeutic potential of immunomodulatory probiotics (immunobiotics) on the attenuation of LF and the underlying mechanisms ameliorating the progression of LF. The results showed that a methionine-choline deficient (MCD) diet resulted in hepatic inflammation, steatosis, increased triglyceride and lipid accumulation, inflammatory immune cells, and fibrosis. Immunobiotics mixtures reduced the MCD-died serum endotoxin, IL-17A, alanine, and aspartate aminotransferase and increased the serum regulatory cytokine and liver weight. Th17 cells, which produce inflammatory cytokine IL-17, on the liver tissues of MCD diet-fed mice were reduced significantly by immunobiotics. The immunobiotics treatment reduced the MCD diet-induced collagen, a-smooth muscle actin, CD68 deposition, and fibrogenic TGF-β signaling activation. The MCD diet reduced gut-barrier integrity, mucin production, and inflammatory cytokines and altered the gut microbiota composition that could be restored by immunobiotics. The administration of immunobiotics increased the aryl hydrocarbon receptors (AhR) pathway activation in both colonic and liver tissues of MCD diet-fed mice.

Conclusions

Our results demonstrate a novel insight into the mechanisms through which immunobiotic administration improves the gut barrier integrity, modulates the gut microbial composition, increases AhR activation, and reduces gut dysbiosis, bacterial translocation, LPS, and inflammatory cytokines levels, which in turn in increases the AhR pathway and inhibits HSCs activation and fibrosis progression beyond the gut in the liver tissue of NASH/LF mice.

Background

High-calorie intake and a sedentary lifestyle increase the prevalence of obesity which has led to the occurrence of fatty liver disease, affecting 25% of the population globally [1]. Fatty liver disease ranges from simple steatosis to non-alcoholic steatohepatitis (NASH), which further progresses to liver fibrosis (LF), cirrhosis, and hepatocellular carcinoma (HCC), leading to liver failure [2]. LF is the primary step toward cirrhotic liver disease and is characterized by the excessive accumulation of extracellular matrix

(ECM) proteins or collagen [3]. Kupffer cells (KCs) are the dominant hepatic macrophage, but the activation of hepatic stellate cells (HSCs), a major producer of ECM proteins, induces the production of proinflammatory mediators and hepatic fibrogenesis [4]. Studies have suggested that the gut–liver axis is a major route of NASH-mediated LF. During gut dysbiosis, the gut-resident microbiota and their endotoxin (lipopolysaccharide) translocate to the liver, where they have been reported to activate both KCs and HSCs via Toll-like receptor 4 (TLR4) and induce inflammation, NASH, and LF [3, 5]. The deficiency of TLR4 attenuates diet-induced NASH and LF in mice [6]. Transforming growth factor (TGF-β) is a key pro-fibrogenic mediator, and it's signaling participates in the progression of LF [5]. Lipopolysaccharide (LPS) administration tends to increase TGF-β production and reduce TGF-β pseudoreceptor BMP and the activin membrane-bound inhibitor (BAMBI) to sensitize HSCs to TGF-β-induced pro-fibrogenic signaling and collagen production [5].

Hepatic infiltrating of the CD4 + T cell subsets, such as regulatory T cells (Treg), T helper 1 (Th1), T helper 2 (Th2), and T helper 17 (Th17) cells, play critical roles in inflammation and fibrogenesis of fatty liver diseases [7, 8]. Treg cells ($Foxp3^+$) control effector T cells and maintain homeostasis and immune tolerance, whereas Th17 cells produce potent inflammatory cytokines (IL-17, IL-21, and IL-22), resulting in induction of inflammatory response [7]. Treg and Th17 cells are the two extremes of the immune response. Therefore, a balance is needed to improve the hepatic complications. The imbalance of Treg/Th17 cells was observed in the liver of mice with NASH [9]. The higher frequency of $IL\text{-}17^+$ cells in the patient's liver and higher ratios of Th17/Treg cells in the peripheral blood indicate the progression from fatty liver to NASH [10]. Neutralization of IL-17 improved LPS induced liver damage [11], and IL-17A deficient mice were resistant to NASH development [12].

The gut microbiota resides in the gastrointestinal (GI) tract of mammals and interacts with the host to provide beneficial functions in several ways [13]. The microbiota influences the differentiation of $CD4^+$ T cell subsets in the intestine [14] and produces numerous metabolites, including dietary tryptophan and butyrate, which act as ligands for the aryl hydrocarbon receptors (AhR) [13, 15]. AhR is a ligand activating transcription factor that plays a vital role in maintaining a healthy gut and intestinal homeostasis [16]. The activation of AhR regulates intestinal intraepithelial lymphocytes, $CD4^+$ T cell subsets, innate lymphoid cells, and AhR target genes, such as cytochrome P450 family 1A1 (CYP1A1), IL-22, and IL-17 [17, 18]. AhR knockdown increased dextran sodium sulfate (DSS) induced colitis in mice [19]. AhR is expressed in colonic tissues and strongly in the liver. A toxic AhR ligand (2,3,7,8-tetrachlorodibenzo-p-dioxin (TCDD) treatment sensitizes mice to diet-induced LF [20], while a nontoxic AhR ligand, 1'H-indole-3'carbonyl-thiazole-4-carboxylic acid methyl ester (ITE), prevent HSC activation and the development of LF in mice [21].

There is no effective treatment for NASH and its associated LF. Therefore, finding natural therapeutic modalities for clinical application against inflammation, NASH, and LF is crucial. The administration of probiotic bacteria maintained colonic barrier functions [22] and attenuated fatty liver diseases, NASH, LF, and HCC development [23, 24]. A probiotic mixture (VLS#3) treatment modulated the gut-microbiota changes, reduced the inflammatory Th17 cells, and promoted anti-inflammatory Treg cells in liver tumors

of mice [23]. The gut-dysbiosis reduced the AhR activity and its ligands [25]. A combination of three probiotics (*Lactobacillus murinus*, *L. reuteri*, and *L. taiwanensis*) could metabolize tryptophan, enhance AhR ligand production, increase IL-22, and reduce colitis and intestinal inflammation in mice [25, 26]. Overall, the studies suggest that maintaining intestinal homeostasis and restoring the gut microbiota and their metabolites are essential for improving NASH and LF. Probiotics administration modulates gut-microbial composition and increases the production of AhR ligands to exert its beneficial effects against colonic diseases. Few studies evaluated the probiotic potential against NASH-mediated LF, but the molecular mechanisms of probiotic action are largely unexplored. This study hypothesized that immunomodulatory probiotics (immunobiotics) might attenuate NASH and LF by modulating the gut microbiota composition and differentiation of $CD4^+$ cell subsets. In addition, this study examined whether immunobiotics improve the gut barrier integrity and AhR activity and reduce hepatic inflammatory and profibrogenic cytokines *in vivo*. Therefore, the efficacy of immunobiotics on the development of NASH and LF in mice fed with a methionine-choline deficient (MCD) diet was evaluated.

Methods

Animal and Experimental Protocol

Six-week-old male mice (C57BL6/6J) were used in this study. The mice were allowed to acclimate for one week on a standard diet (SD) and were divided into six groups and housed in individual cages under pathogen-free conditions on a 12/12h day/night cycle. All groups of mice (n= 9-12/group) were fed either SD or methionine-choline-deficient (MCD) diet *ad libitum* for 10 weeks. Group 1 (negative control) received the SD. Group 2 (positive control) was fed the MCD diet to establish the animals for diet-induced NASH and LF. Groups 3 and 4 (Preventive model) were fed the MCD and received live and heat-killed immunobiotics (1×10^9 cells/Mouse/Day) orally from 0–10 weeks. Groups 5 and 6 (Treatment model) were pre-fed a MCD diet and then given live and heat-killed immunobiotics (1×10^9 cells/Mouse/Day) orally from 4–10 weeks. All animals received human care, and all study protocols were approved by the animal ethics committee of Dongguk University. The weights of the mice were measured from 0–10 weeks.

Preparation of immunobiotics

A mixture of live and heat-killed immunomodulatory probiotic strains was used. The mixture contained a combination of three probiotic strains, such as *Lactiplatibacillus plantarum* DU1, *Levilactobacillus brevis*, and *Weissella cibaria* DU1, which were selected based on their anti-inflammatory, anti-viral, and anti-hepatic steatosis activities *in vitro* [27, 28]. The selected probiotics were cultured in De Man-Rogosa-Sharp (MRS) broth at 37°C. After 15 h incubation, the cells were centrifuged at 4000 rpm for 10 minutes, washed with distilled phosphate-buffered saline (DPBS), and suspended in PBS at the concentration of 1×10^9 colonies. A set of probiotics mixtures was then heat-killed by incubating at 70°C for 1h and stored at -80°C for further oral administration into the mice.

Stool, serum, and tissue samples preparation and in vivo permeability assay

At the end of the experimental period, fecal samples were collected from each group of mice before sacrifice. The *in vivo* intestinal permeability was examined using an FD4 assay. The FD4 (Sigma) was administered (6mg/10g body weight) to the mice, and whole blood was collected after 3 h to analyze the fluorescence intensity of FD4 using a plate reader. Once the mice were anesthetized, the blood was collected from the inferior vena cava. The serum was separated by centrifugation and stored at -80°C. The weight of the liver and spleen and the intestinal length were measured immediately after excision from the mice, snap-frozen in liquid nitrogen, and stored at -80°C. The samples were then fixed with 4% formalin and stored at 4°C for further analysis.

Cell isolation and preparation

To isolate the lymphocytes from the mouse liver, the mice were anesthetized. The hepatic portal vein was cannulated with a 25-gauge needle, and the liver was perfused with ice-cold PBS/ethylene glycol tetraacetic acid (EGTA) for 5 min, followed by prewarmed collagenase D/DNaseI solution for 5 min. The liver was then removed to a Petri dish, smashed by adding RPMI medium, and filtered through a 70 mm cell strainer. The total cell suspension was centrifuged at 50 × g for 1 min to remove the parenchymal cells, and the supernatant was transferred to a fresh tube and centrifuged at 500 × g for 8 min at 4°C. The pellet with the parenchymal cells was then resuspended in 10 ml of RPMI medium containing 37.5% percoll and 100 U of heparin and centrifuged at 1500 × g for 20 min at 4°C. The cells were then resuspended with FACS buffer or RPMI medium.

FACS analysis

Fc-blocked intrahepatic mononuclear cells ($1–5 \times 10^6$) were plated in a 96 well plate and surface stained with CD45, CD3, CD4, $CCR2^+$, and CD25 (Table 1) and treated with a FoxP3 transcription factor fixation/permeabilization solution (eBioscience) prior to intracellular staining of the nuclear protein with Foxp3. The cells were stimulated with a cell stimulation cocktail (eBioscience) for 14–16 h in an incubator at 37°C under an atmosphere containing 5% CO_2. The cells were then surface stained, followed by intracellular staining of the cytoplasmic proteins, such as IL-17A, IL-10, IL-4, and IFNG (eBioscience). All antibodies were used according to the manufacturer's instructions. FACS analysis was performed using a cytoFlex flow cytometer (Beckman Coulter Life science, IN, USA).

Biochemical assays

The serum endotoxin levels were analyzed using Pierce Limulus Amebocyte Lysate (LAL) chromogenic endotoxin quantification kit (Thermo Fisher Scientific, MA, USA) according to the manufacturer's instructions. The serum oxaloacetic transaminase (GOT), glutamic pyruvate transaminase (GPT), and liver triglyceride (TG) levels were determined using an enzymatic assay kit (Asan Pharmaceutical Co., Seoul, South Korea).

Enzyme-linked immunosorbent assay

The IL-17A and IL-10 levels in the serum were determined using mouse IL-17A and IL-10 ELISA kits, respectively (Invitrogen, MA, USA) according to the manufacturer's instructions.

Histopathological analysis

The colon and liver tissues from the mice were fixed, dehydrated, and embedded in paraffin. The colonic histological sections were cut and stained with hematoxylin-eosin (H&E), alcian-blue (Alcian blue PAS staining kit, Abcam, Cambridge, UK), and picro-sirius red stain (Abcam, Cambridge, UK). The liver tissue sections were stained with H&E to assess steatohepatitis and with picro-sirius red stain to analyze hepatic collagen deposition. The frozen sections of liver tissues were also stained with Oil-Red O (Sigma–Aldrich, USA). The stained tissue sections were examined using an Olympus BX53 microscope (Olympus, Japan).

The colonic and liver histological sections were subjected to immunohistochemical staining with different antibodies. The colonic sections were incubated with anti-ZO-1, anti-Occludin, and anti-HuD antibodies (Cell signaling Technology, Beverly, MA, USA), while liver sections were incubated with anti-a smooth muscle actin (a-SMA), anti-CD60 (Cell signaling Technology, Beverly, MA, USA), and anti-AhR antibodies (Abcam, Cambridge, UK). The brain tissue sections were incubated with anti-HuD (Cell signaling, MA, USA), anti-GFAP, and IbA1 antibodies (Abcam, Cambridge, UK).

Quantitative Real-time Polymerase Chain Reaction

The RNA from the frozen colonic and liver tissues was extracted by adding TRIZOL reagent. The purity and quantity of RNA were analyzed using the Nanodrop method (NanDrop Technologies, USA), and the cDNA was synthesized using a thermal cycler (BIORAD, Hercules, CA, USA). RT-PCR was performed using a 7300 real-time PCR system (Roche Applied Science, Indianapolis, ID, USA) with SYBR green and specific primer sets. The volume of the reaction mixture was 20 µl, which contained 1 µl of cDNA and 19 µl of master mix, including SYBR green and the forward and reverse primers (1pmol/µl). The amplification was performed at 50°C for 5 min; followed by 95°C for 5 min; then 40 cycles at 95°C for 15s, 60–63°C for 30s, and 72°C for 30s. β-actin was used as an internal control.

Western blot analysis

The colonic and liver tissues were homogenized and dissolved in RIPA buffer. The concentration of protein in the lysed sample was analyzed using a bicinchoninic acid (BCA) assay kit (Thermo Scientific, Pierce, Rockford, IL). The samples were heated to 95°C for 5 min, separated using SDS-polyacrylamide gels, and transferred to a nitrocellulose membrane (Trans-Blot Turbo^{TM}, BIO-RAD). The transferred membrane was cut at the desired part and incubated with a blocking buffer, followed by incubation with the appropriate primary antibodies. Goat anti-rabbit and anti-mouse IgG-HRP antibodies (Cell signaling Technology, Baverly, MA, USA) were used as the secondary antibodies. The optical protein bands were

detected by adding a mixture (1:1 ratio) of western blot detection solutions A and B (SUPEX, Neonex Co., Ltd, Postech, South Korea). The area of the densitogram peak was estimated using Image J software (National Institute of Health, Bethesda, MD, USA).

Gut microbiota analysis

Mice fecal samples were collected and stored immediately at -80°C. The total DNA from the fecal samples was extracted using a QIAam fast DNA stool mini kit (QIAGEN, Hilden, Germany) according to the manufacturer's instructions. The microbial 16S rRNA V_1–V_3 region was amplified using a C1000 Touch thermal cycler (Bio-rad, Hercules, CA, USA). The amplicons were purified using a QIAquick PCR purification kit (QIAGEN, Germany). The concentration of amplicons was quantified using a PicoGreen dsDNA assay kit (Invitrogen, Carlsbad, CA, USA). The amplicons were amplified by emulsion PCR and sequenced using a Roche/454 GS Junior system (454 Life Sciences, Branford, CT, USA). The sequences were sorted using a barcode in the demultiplexing step to reduce error, and low-quality reads (average quality score < 20 or read length <300 bp) were eliminated for analysis. The sequences were then processed and clustered into operational taxonomic units (OTUs) at 97% similarity. Subsequently, the representative sequence of each OTU was selected using a Quantitative Insights into the Microbial Ecology (QIIME) software package [29]. The total structural changes in the microbial community were analyzed by UniFrac-based principal coordinate analysis (PCoA). A web-based program was used to analyze Lefse [30]. Heatmap was created using R and R studio programs. The relative abundance of gut microbiota was represented as a percentage.

Study of AhR activity

The AhR activity of the mice stool samples was analyzed using a luciferase reporter assay, according to the method described elsewhere [15, 25]. Briefly, HT-29 and LX-2 cells that contained xenobiotic response elements luciferase reporter plasmid (pGL4.43[luc2P/XRE/Hygro]) were seeded (3×10^4 cells/well) in 96 well and small tissue culture (6mm) plates and stimulated with stool samples suspensions (1:10 ratio) for 24 h. The luciferase activity was measured as relative luminescence units using a microplate reader. The values were normalized on vehicle-treated cells, and the results are expressed as the fold changes. The western blot was also performed to analyze the level of AhR related proteins (AhR, Cyp1a1, and Cyp1b1) *in vitro*.

Statistical analysis

GraphPad Prism 8.0 (San Diego, CA, USA) and SPSS software package (SPSS 12.0, SPSS Inc., Chicago, IL, USA) were used to analyze the samples and produce graphs. The groups were compared by one-way analysis of variance (ANOVA) followed by a post hoc Tukey multiple comparisons test. The results are presented as the mean ± SEM and *P*-values < 0.05 were considered significant.

Results

Immunobiotics feeding ameliorates MCD diet-induced NASH and LF in mice and is dependent on the gut permeability, gut microbiota, and AhR

The widely accepted methionine/choline-deficient (MCD) diet model that induces NASH and liver fibrogenesis in mice were used to determine the therapeutic potential of immunobiotics [31]. The mixture of three immunobiotic strains (live and heat-killed) was orally administrated from 0 day of MCD diet feeding (PL and PK) or after four weeks of MCD diet feeding (TL and TK) (Fig. 1A). The MCD diet-fed mice showed a significant decrease in body weight, liver and spleen weights, and an increase in the liver triglycerides (TG), serum GOT, and GPT levels. In contrast, the immunobiotic-fed mice showed significant improvement in their weights and a decrease in the liver TG and GPT (Fig. 1B). Mice fed the MCD diet developed micro and macrovascular steatosis and inflammation and increased NASH score and lipid accumulation in the liver (Fig. 1C and D). The liver sections from the mice administered immunobiotics (PL, PK, TL, and TK) had lower pathophysiological pictures of NASH than the MCD diet-fed mice. The PK group showed better results than the other groups. Feeding the MCD diet also led to significant increases in LF, which is characterized by increased collagen deposition, a-smooth muscle actin (a-SMA), and CD68 expressing KC and macrophages. (Fig. 2A and B). Collagen deposition and a-SMA are the staple markers for developing fibrosis and the activation of HSCs in the liver [3, 5]. The coadministration (PL or PK) immunobiotics had a significant effect on the reduction of MCD induced LF and the mRNA level of pro-fibrogenic markers, such as Col1A1, a-SMA, MMP-9, TGF-b, and TIMP-1 (Fig. 2A-C). The levels of these markers, except for MMP-9 in the TL and TK group, were significantly lower than in the MCD diet-fed group.

Immunoblotting analysis revealed the level of a-SMA to be higher in the liver samples of the MCD fed mice, but it was reduced by immunobiotics administration (Fig. 2D). Changes in the a-SMA protein levels were similar to the changes in the a-SMA mRNAs (Fig. 2C) and a-SMA immunostaining (Fig. 2A). Previous studies suggested the infiltration of hepatic T-helper (Th) cells during NAFLD and NASH development [8, 24]. Th17 cells with the specific IL-17 cytokine led to tissue inflammation and recruited leukocytes, which are reported to be higher in the NASH patients and NASH mice [11, 32]. Therefore, this study examined whether immunobiotics would modulate the frequencies of liver infiltrating Th17 cells and Treg cells in mice. The Th17 and T cells were measured by gating the singlets for $CD45^+$ cells, followed by gating for CD4 cells. The frequencies of the IL-17-producing CD^+T cells were higher in the liver tissues of the MCD-fed mice but lower in the immunobiotic fed groups (PL, PK, TL, or TK) mice (Fig 2 E). The mice fed the immunobiotics (PL or PK) showed a higher percentage of Treg, Tr1, and Th2 cells and a lower percentage of Th1 and $CD3^+CCR2^+$ cells than the MCD fed mice. This result suggests that the reduction of NASH-mediated liver fibrogenesis in the MCD diet-fed mice might be associated with the decreased infiltration of Th17 cells and increased infiltration of Treg cells.

In addition, to determine if the reduction of hepatic fibrogenesis in the immunobiotic-fed mice groups may cause by regulating the fibrogenic TGF-b signaling, the proteins associated with the TGF-b/Smad pathway in the liver tissues of mice were analyzed by western blot. Mice fed the MCD diet exhibited higher profibrogenic cytokine TGF-b levels than the chow-fed control group. Interestingly, immunobiotic

administration (all groups) downregulated the TGF-b level in the liver tissues of mice to remarkably lower levels than in the MCD-fed mice groups (Fig. 2F). The phosphorylation of Smad3 was also down regulated in the immunobiotic-fed mice groups. A higher level of Smad7 was also observed in the liver tissues of the mice fed immunobiotics (Fig. 2F), suggesting that the immunobiotics beneficially modulated the TGF-b/Smad pathway to ameliorate the development of hepatic fibrogenesis in the NASH mice.

With regard to the inflammation-associated markers, the hepatic IL-17A, CCL5, TNF-a, IL-1b, CCL2, and TLR4 mRNA levels were higher in the MCD diet-fed mice than in the chow diet-fed mice groups (Fig. 3). The coadministration (PL or PK) immunobiotics significantly down regulated the expression of MCD-induced liver inflammatory markers and produced a higher level of anti-inflammatory cytokine IL-10 than MCD groups. In addition, MCD fed mice had higher liver mRNA levels of fibronectin, desmin, ICAM-1, MMP-2 and macrophage activation (YM-1), and fibroductular markers (K7, K19, and Sox9) (Fig. 4A and B). These changes were similar to the reports for mouse NASH livers [33]. Immunobiotic (PL, PK, TL, or TK) administration reduced the mRNA levels of ICAM-1 and Col1A2, and YM-1) and K19 than the MCD diet-fed mice (Fig. 4A and B), while there was no significant reduction found in the levels of desmin and Sox-9.

Immunobiotics alleviate the MCD diet-induced pathological changes in the intestine of mice

The liver tissue examination confirmed the protective role of immunobiotics, but it was unsure how the immunobiotics mediate their protective effects on hepatic fibrosis in mice. The loss of intestinal barrier integrity, increase in intestinal permeability, gut dysbiosis endotoxemia, and small intestinal bacterial overgrowth are standard features of NASH [34, 35]. Therefore, it was hypothesized that administering immunobiotics would improve the intestinal damage caused by the MCD diet in mice. At the end of MCD diet feeding, the length of the colon was shorter than chow diet-fed control mice (Fig. 5A). The mice fed the immunobiotics showed a significant increase in colonic length than the MCD diet-fed mice. The H&E histological examination revealed remarkable changes in the colonic structure of the MCD diet and immunobiotic-fed mice groups (Fig 6A). The colonic tissue of the control mice showed a normal morphological structure with intact mucosa and muscular layers. The mucosal layers were compact with clear crypt and goblets cells, and muscular layers were conserved without the infiltration of leukocytes (Fig 6A). The myenteric ganglia were full of neurons (Fig. 5B). The infiltration of leukocytes, eosinophils, no clear crypts, and loss of goblets and HuD positive neurons were observed in the colonic tissues of mice that fed the MCD diet. The colonic tissues of immunobiotic-fed mice showed a similar morphological pattern to that observed in the control mice. Collagen deposition and the mRNA level of Col1A1in the colonic tissues of the MCD-fed mice were lower than in control and immunobiotic-fed mice groups (Fig. 5C and D). The goblet cells density in the colon are important for maintaining the production of mucus and glycoproteins (mucins) that are dispersed widely throughout the mucosal epithelium and play roles in nutrient transport and epithelial cell protection [36]. Alcian blue (AB) and periodic acid-schiff (PAS) staining are widely used to stain mucins. Therefore, the acidic and neutral mucins were stained magenta in the colonic tissues of mice. AB-PAS straining showed that the MCD diet-fed mice had a low

density of goblet cells with the depletion of mucus production compared to the control (Fig. 6B). The MCD diet mediated depletion was improved when the mice were fed the immunobiotic food. These results suggest that immunobiotic feeding improves the MCD diet-induced intestinal pathology in the mice.

Immunobiotics reduced the MCD diet-induced intestinal permeability and bacterial translocation in mice

Based on the colonic histology results, it was hypothesized that immunobiotics feeding would improve the intestinal barrier integrity in the MCD diet mice. An *in vivo* permeability assay was performed using FD4. The MCD diet increased the intestinal permeability, which was reduced by immunobiotic feeding (Fig. 6C). The intestinal barrier integrity is controlled by tight-junction proteins, mainly zonula occludens (ZO)-1, claudin-1, and occluding-1 [24]. The mRNA level of ZO-1, claudin-1, and occluding-1 were lower in the colonic tissue of the mice fed the MCD diet (Fig. 6C). As shown by the IHC and western blot study, a decrease in the level of these proteins was also observed in the colonic tissues of the MCD diet-fed mice compared to control and immunobiotic-fed mice (Fig. 6D-F). The PK group of mice had a higher ZO-1, claudin-1, and occluding-1 expression than the other immunobiotic groups (Fig. 6C). By contrast, the PL group of mice showed these proteins at a higher level than the other groups (Fig. 6E). The mice pre-treated with viable or heat-killed (HK) immunobiotic also increased the level of the TJ proteins before MCD diet feeding, but not higher than the PL and PK groups. Furthermore, this study investigated whether the MCD diet-induced intestinal permeability would increase the bacterial translocation to the liver tissue of the mice. The mice fed with the MCD diet exhibited gut bacterial translocation into the liver tissues (Table S1). The administration of immunobiotics impeded bacterial translocation. Only two of the five mice received viable immunobiotics (PL), and three of the five mice that received the other groups (PK, TL, TK) showed culturable bacteria. The chow diet-fed mice had no culturable bacteria in the liver tissue. These results suggest that using viable or heat-killed immunobiotics increased the TJ proteins to improve the intestinal barrier integrity and reduce the bacterial translocation in mice with MCD diet-induced LF.

Immunobiotics reduced serum endotoxin and Th17 levels and other inflammatory markers in mice

Previous studies reported that gut-derived endotoxin plays a critical role in inducing liver injury, particularly in the development and progression of NAFLD, NASH, and hepatic fibrogenesis [22, 37]. Gut-derived LPS translocate into the liver via portal circulation and activate TLR4 in the liver cells, resulting in the development of NASH and fibrosis [5]. The probiotic treatment reduced the serum endotoxin level and improved the gut-barrier integrity in the mice with choline-deficient/L-aminoacid-defined (CDAA) diet-induced NAFLD [37]. The mice fed the MCD diet had significantly higher serum endotoxin levels than the control mice (Fig. 6G). The immunobiotic (PL, PK, TL, or TK) treatment significantly reduced the endotoxin level in the serum of mice. There were no remarkable differences between the immunobiotics-fed mice groups. In addition, a significant increase in the serum and colonic mRNA levels of Th17 was observed in the MCD diet-fed mice compared to the control mice, but these increases were reduced significantly when the mice were fed the immunobiotics (Fig. 6G). In contrast, the immunobiotics treatment (PL or PK) elevated the serum and colonic mRNA expression levels of IL-10 in mice with MCD

diet-induced LF (Fig. 6G). The other immunobiotics-fed group (TL or TK) mice also had a higher level, but not significantly, than the MCD-fed mice. Furthermore, the expression of other proinflammatory cytokines in the colonic tissues of mice was analyzed. The MCD diet increased the mRNA level of IL-6 significantly compared to the control mice (Fig. 6H). On the other hand, immunobiotic administration decreased the MCD diet-induced IL-6 expression in the colonic tissues of the mice but did not significantly down-regulate the mRNA level of TNF-a, IL-1b, and CCL2 compared to the MCD diet. The MCD diet upregulated the mRNA level of TLR4 significantly, but these were reduced by immunobiotics (Fig. 6H). Hence, the administration of immunobiotics reduced the serum and colonic inflammatory biomarkers by improving the intestinal barrier integrity or reducing intestinal permeability in mice with MCD diet-induced LF.

Immunobiotics modulated gut microbiota in mice with MCD diet-induced liver fibrosis

Several studies reported that the severity of fatty liver diseases is associated with the gut microbiota dysbiosis in humans and animals [38, 39]. Changes in the gut microbial composition were also observed in mice fed with a high-fat diet (HFD) and MCD diet [40, 41]. Therefore, it was hypothesized that the administration of immunobiotics would restore the changes in the MCD diet-induced gut microbiota in mice. The structural composition of the gut microbiota was determined by 16S rRNA sequencing of fecal samples from different groups of mice. A principal coordinate analysis (PCoA) based on the UniFrac unweighted and weighted showed that the structures of the microbial community segregated differentially among the groups (Fig. 7A and Fig 1SA). The MCD and immunobiotics fed groups were separated completely from the control group. The clusters of immunobiotic groups (PK and PL) were separated from the MCD groups, while the TK and TL groups formed clusters that were not completely distinct from the MCD group**.** These results suggest that the MCD diet induced a profound shift that could be restored using immunobiotic bacteria. The rarefaction curves reflected that the immunobiotic (PK and PL) fed groups were more diverse than the MCD fed group, while the TK and TL fed groups were not more diverse (Fig. 1SB). The MCD diet reduced the gut microbiota a-diversity metrics compared to the control and immunobiotic groups (PL and TL) (Fig 7C and D). The gut microbiota of all groups was classified as phyla, family, and genera that were different between the groups. The *Bacteroidetes*, *Firmicutes*, and *Proteobacteria* were the three dominant phyla observed in all groups. The relative abundance of the phyla, *Bacteroidetes* and *Firmicutes,* were similar in the MCD and chow diet-fed control groups (Fig 7D, Fig 1SC, and D), which is consistent with an earlier report [38]. On the other hand, *Proteobacteria* was lower in the MCD diet group than in the control group. Boursier et al. [39] reported similar results for patients with NASH and without NASH. Compared to the MCD group, an increase in the abundance of *Bacteroidetes* and *Proteobacteria* and a decrease in the abundance of *Firmicutes* and observed in immunobiotic fed groups (PK, PL, and TK). At the family level, MCD diet-fed mice had a higher abundance of *Bacteroidaceae*, *Rikenellaceae*, *Lactobacillaceae*, *Turicibacteraceae*, and *Erysipelotrichaceae* and a lower abundance of S24-7, *Clostridiales*, *Lachnospiraceae*, *Ruminococcaceae*, and *Prevotellaceae* compared to the control group (Fig. 7E). Similarly, the abundance of fibrosis-associated *Ruminococcaceae* was decreased when fibrosis could become more severe in non-obese individuals[42]. Nevertheless, immunobiotic administration altered the pattern of the bacterial abundance

at the family level compared to MCD groups. At the genus level, compared to the control group, the relative abundance of *Bacteroides, Parabacteroides*, *Lactobacillus, Allobaculum*, and *Turicibacter* were higher, whereas *Ruminococcus*, *Coprococcus,* and *Prevotella* were significantly lower in the MCD groups (Fig. 3SA and B). Similar results were observed in the non-obese subjects with severe fibrosis. The administration of *Ruminococcus* alleviates liver damage in NAFLD mice fed with the MCD diet [42]. On the other hand, immunobiotic groups (PL and PK) had a different pattern of gut microbiota at the genus level than the MCD group, suggesting that immunobiotic feeding beneficially alters the gut microbiota to protect against fibrosis.

In addition, specific taxa that respond to MCD diet and immunobiotic administration were examined using the LDA effect size (LEfSe) assay to determine the differences in the microbial abundance among the groups and each other. The results showed that 55 microbial taxa at the genus level were identified as markers that discriminate the gut microbiota among the groups (Fig. 7F, Fig. 3SA). In the MCD group, the microbial taxa changes after the MCD diet were dramatic compared to the chow diet-fed control group. Interestingly, immunobiotic-feeding groups had different genus levels of microbial taxa compared to the MCD group. In particular, *Lactobacillales* and *Lactobacillus*, which belong to the family *Lactobacillaceae* and phylum *Firmicutes*, may play a role in alleviating the development of fibrosis, were higher in the PK group compared to the MCD group. In contrast, *Bacteroides* in phylum *Bacteroidetes* were enriched in the PL group, while the abundance of *Erysipelotichia* (a producer of short-chain fatty acid) in phylum *Firmicutes* was higher in the TL group compared to the MCD-diet group. The number of microbial taxa was different when compared with each other (Fig. 3SB-F, Fig. 4SA-E).

This study examined the correlation of the gut microbiota with the disease markers to study the impact of the gut microbiota on disease. The abundance of *Lactobacillus* and *Allobaculum* (higher in PK and TL groups) was positively associated with body weight and liver and spleen weight (Fig. 7G). In addition, a genus *Bacteroides* enriched in the immunobiotic groups had a positive association with the body weight and liver weight. Moreover, the abundance of *Odoribacter* was positively correlated with the body weight, liver, and spleen weight and negatively correlated with the liver TG, GOT, GPT, and serum endotoxin. By contrast, *Prevotella* (lower in the MCD diet-fed group) and *Suttrella* were negatively correlated with the body weight, liver, and spleen weight, while positively correlated with the GOT, GPT, and serum endotoxin levels. *Coprococcus* and *Ruminococcus* were lower in the MCD diet-fed group. They had a moderate negative correlation with body weight, liver, and spleen weight and a moderate positive correlation with the serum endotoxin and GPT levels (Fig. 7G). The genus *Oscillospira* had a strong negative correlation with the liver TG, GOT, GPT, and serum endotoxin levels. Previous studies showed that the MCD diet lowered the body, liver, and spleen weights, and increased the liver TG, GOT, GPT, and serum endotoxin levels, which are major risk factors for liver injury by inducing inflammation in the host [37, 43]. A strong correlation was observed between these factors and the gut microbiota, which may participate in the development of LF.

Immunobiotics activated AhR in the colonic and liver tissues of mice and *in vitro* cells

Overall, immunobiotics modulate the MCD diet-mediated gut microbiota in mice, but it is unclear how the modulation of gut microbiota by immunobiotics would alleviate LF. Studies reported that the expression of AhR, production of AhR ligands, and AhR pathway activation are reduced in the gut of patients with intestinal diseases [26]. Modulation of the gut microbiota by *Lactobacillus* increased the production of AhR ligands and AhR activation, which alleviated the intestinal pathology in mice [26]. The production of sufficient AhR ligand is critical for restoring the composition and function of the gut microbiota [44]. AhR signaling protected against intestinal diseases and prevented HSC activation and liver fibrosis in mice [21]. Therefore, this study next examined whether immunobiotics feeding increases the expression of AhR and AhR signaling activation in both intestinal and liver tissues of mice. Interestingly, the protein and mRNA levels of AhR and its signaling proteins (Cyp1b1 and Cyp1a1) were higher in the colonic tissue of mice fed the immunobiotics than in the MCD diet alone (Fig. 8A and B). A similar pattern of AhR and other proteins was found in the AhR colonic cells treated with fecal extracts derived from mice fed the immunobiotics (Fig. 8C). AhR activity was found to be increased in HT-29 cells treated with feces from PL and PK group of mice (Fig. 8C). Furthermore, the mRNA levels of these proteins were higher in the liver tissue of the immunobiotic-fed mice groups (Fig. 8D). On the other hand, AhR at the protein level was higher in all immunobiotic groups, while Cyp1a1 and Cyp1b1 were lower in the PL group compared to the MCD group (Fig. 8E). An *in vitro* study also showed a similar pattern of AhR protein in LX-2 cells incubated with a fecal extract from the immunobiotic-fed mice groups (Fig. 8G). An immunohistochemistry study showed that the liver tissues of mice administered with immunobiotics had higher AhR positive cells than the MCD group (Fig. 8F). These results suggest that immunobiotics positively modulated gut microbiota to produce a higher level of AhR ligands and AhR pathway activation, which may play a crucial role in reducing LF in the MCD diet-fed mice.

Discussion

The immunobiotics treatment prevented the progression of MCD diet-induced NASH to LF in a mouse model. The oral administration of immunobiotics improved the gut barrier integrity, reduced bacterial translocation and inflammatory cytokines, and modulated the gut bacterial composition. Furthermore, the immunobiotics reduced the pro-fibrogenic markers and pathological scores, influenced immune cell differentiation, and activated the AhR markers in the liver tissue of mice. These results highlight the importance and therapeutic potential of immunobiotics in treating liver diseases.

MCD diet-induced NASH is a widely accepted model that mimics human NASH. An MCD diet intake induces inflammation, lipid accumulation, steatohepatitis, and fibrosis in the liver tissues of mice, which results in a loss of body and liver weight and elevated gut-derived endotoxin in the portal circulation [45, 46]. An increase in endotoxemia induces inflammatory cytokines, which results in hypoxia-ischemia in the intestinal mucosa and further increases the intestinal permeability [47]. The permeability of LPS into the portal circulation induces a systemic inflammatory response and hepatic injury, leading to HSC activation that increases α-SMA and collagen deposition, resulting in liver NASH and LF [48]. The mice injected with LPS showed extensive hepatic damage and reduced colonic barrier function [22]. An increase in intestinal permeability was reported to induce an elevation of the serum LPS and correlate with the severity of

NAFLD in children [49]. Hence, an improvement in intestinal function is vital for preventing hepatic fibrosis. The oral administration of VSL#3 does not reduce the MCD diet-induced serum endotoxin level significantly in mice [45]. The immunobiotics treatment reduced serum LPS level and intestinal permeability significantly and increased mucin production and the ZO-1, occludin, and claudin-1 levels in the colonic tissue of MCD diet-induced hepatic fibrosis mice, which is in agreement with the results reported by Endo et al.[37]. Similarly, *Lactobacillus* GG administration reduced the level of gut-derived endotoxins in the portal circulation and lipid accumulation and inflammation in the liver of the NAFLD mice model [50]. IL-17A promotes inflammation by inducing the production of inflammatory cytokine/chemokines in the affected tissues [32]. The MCD diet tended to increase the serum and mRNA levels of IL-17A while reducing the IL-10 that exhibited anti-inflammatory and immunosuppressive effects in the colonic tissues of mice [32]. The MCD diet also increased the gene expression of IL-6, IL-1β, and TLR4 in the colonic tissues of mice [51]. The oral administration of immunobiotic mixtures reduced the serum IL-17A, mRNA levels of IL-6, IL-1β, and TLR4 in the colon of the MCD diet-fed mice. The decreased colonic cytokine expression and bacterial translocation in the immunobiotic-treated groups are probably due to the improvement of immunobiotic-mediated gut barrier function and reduction of LPS production [52].

The gut-liver axis plays a crucial role in liver pathogenies, and probiotics beneficially modulate the gut-liver axis and pathological markers associated with NASH and hepatic fibrosis [24, 41]. The higher AST and ALT levels in the serum, the pathological changes, and the higher level of triglycerides in the liver denote hepatic tissue damage [53]. The oral administration of immunobiotics reduced the AST and ALT levels, hepatic steatosis, and inflammation scores in the mice fed with the MCD diet, which is consistent with the results reported elsewhere [54]. Another report using *L. lactis* and *Pediococcus pentosaceus* showed similar AST and ALT levels and liver pathology scores [55]. The activation of TLR signaling in the immune cells of the liver tissues produce an array of proinflammatory cytokines that could disrupt the gut barrier integrity and increase bacterial translocation, resulting in secondary activation of TLR signaling [56]. The results showed that immunobiotic mixtures reduced TLR4 expression, which was higher in the liver tissues of the MCD fed mice. TLR4 signaling participates in the progression of NASH and LF, and its absence in mice has less fibrosis induced by carbon tetrachloride [5, 57]. A previous study reported that TLR4 signaling on HSCs, but not on hepatocytes and KCs, is important for LF5. KCs are the primary cells that respond to gut-derived LPS to produce IL-1β, TNF-□, CCL2, and IL-10 [58]. The production of these cytokines is involved in hepatic inflammation and its associated dyslipidemia [59]. The immunobiotics treatment reduced the proinflammatory cytokines, such as TNF-□, CCL2, and IL-17A, and increased IL-10 expression in the liver tissues of mice. In addition, the percentage of CD68 cells was also lower in the liver tissue of mice that received the immunobiotics mixture, suggesting that immunobiotics alleviate KCs cells activation and its associated inflammation.

HSCs are another key mediator of the gut–liver axis, producing proinflammatory and pro-fibrogenic markers in response to LPS[5]. TLR4 signaling crosstalks with TGF-β signaling, a potent pro-fibrogenic mediator in HSCs. TLR4/LPS signaling in KCs secretes TGF-β, which actively differentiates quiescent

HSCs to fibrogenic HSCs, resulting in the production of pro-fibrogenic factors and LF progression [5]. Previous studies showed that an MCD diet induces the production of pro-fibrogenic markers, such as col1A1, α-SMA, MMP-9, TGF-β, and TIMP-1 [45, 46, 51]. In the present study, the same trend of an increase in fibrogenic markers was observed in the liver tissues of mice fed with the MCD diet alone. The increased expression of col1A1, α-SMA, MMP-9, TGF-β, TIMP-1, and ICAM-1 induced by the MCD diet were reduced significantly by immunobiotics [45, 54].

The inflammatory response underlying NASH and LF is characterized mainly by the increased production of inflammatory cytokines/chemokines and infiltration of inflammatory and regulatory T cells [32, 60]. The regulatory T cells (Treg) play a critical role in regulating the inflammatory process in NASH and LF, while T helper cells 17 (Th17) have an opposite role in NASH development. The patients with NASH had significantly higher infiltrates of Th17 cells and lower infiltrates of Treg cells [10, 11]. The Treg/Th17 imbalance is important for regulating NASH and LF progression. The MCD diet induced NASH development in mice and increased the infiltration of Th17 cells [32]. The Th17 cells are the primary source of IL-17 secretion, and the elevated level of IL-17 exacerbates hepatic inflammation and steatosis in mice with NASH and NAFLD [11, 32]. IL-17A upregulates the expression of profibrotic genes by activating the TGF-β receptor on HSCs in a JNK-dependent approach [61]. IL-17-deficient mice showed a lack of NASH development [32]. IL-17 signaling was critical for the progression of LF in the bile duct ligation and CCl4-treated mice model [62]. An increase in the frequency of Th17 cells was observed in the MCD diet-fed mice, suggesting that Th17 cells and IL-17A production affect the LF progression [9]. On the other hand, the percentage of inflammatory Th17, Th1, and $CCR2^+$ cells infiltrations were reduced significantly in the immunobiotic treated mice groups. In addition, mice that received the immunobiotics (except the TL group) had a higher percentage of immunoregulatory Treg cells than the MCD diet-alone feeding groups [63]. The neutralization of IL-17 and dominance of Treg cells were from NASH and LF progression [9, 64]. These results provided insights into the regulation of inflammatory and regulatory immune cell infiltration into the inflamed liver tissues via the gut–liver axis.

Studies showed that the gut–liver axis, a bidirectional relationship between the gut and liver diseases, and the gut microbial composition represent vital factors in NASH and LF progression [24]. Gut dysbiosis is associated with liver diseases and aggravated disease severity [24]. NASH patients had a different pattern of gut microbiota composition than the healthy subjects, suggesting an emerging role of the gut microbiota in NASH and LF progression [39, 42]. The germ-free mice that received gut microbiota from NASH patients showed exacerbated hepatic inflammation, steatosis, and fibrosis [65]. Hepatic lipid accumulation, inflammation, and HCC formation were observed in the germ-free mice with fecal microbiota from the high-diet induced mice [66]. These studies suggest a direct role of the gut microbiota in developing and progressing liver diseases, including NASH and LF. Depletion of the gut microbiota by antibiotics in mice had reduced levels of LPS and fibrogenesis formation, suggesting that the gut microbiota is the primary source of LPS production and LF progression [5]. Restoration of an altered gut microbiota is crucial for preventing NASH and LF progression. Many studies showed that probiotic bacteria could positively modulate or restore the gut microbiota balance [67]. These results showed that

immunobiotics-fed mice had a different gut microbial composition than the microbial pattern observed in the mice fed the MCD diet alone. The proportional ratio of the *Firmicutes* and *Bacteroidetes* plays crucial roles in developing diseases, including liver diseases. The immunobiotic-treated MCD diet groups had a greater abundance of beneficial bacteria, such as genus *Bacteroides*, *Prevotella* (PK and PL group), and *Helicobacter* (PK and TK group), which are producers of short-chain fatty acids (SCFAs), particularly propionate, which improve the gut barrier integrity and gut homeostasis [68, 69]. *Ruminococcus* is a key bacterium that maintains gut homeostasis in healthy subjects [42]. A lower level of *Ruminococcus* was associated with NAFLD and the worsening severity of fibrosis in NAFLD patients [70]. The lower abundance of genus *Ruminococcus* in the MCD diet group was increased by immunobiotics, suggesting that immunobiotics beneficially modulate the gut microbiota in an MCD diet.

Previous studies reported that the increases in the level of SCFAs alleviate chronic inflammatory, metabolic, and liver diseases [24]. Certain gut microbiota increases the production of SCFAs, which act as a ligand for AhR [15]. In addition, gut microbiota-derived indole is also a ligand for AhR, and activation of the AhR pathway reduces intestinal inflammation and the severity of celiac disease [26] and metabolic diseases [71]. The production of nontoxic AhR agonists prevented the activation of HSCs and reduced liver fibrogenesis in mice21. NOD/DQ8 mice gavaged with *L. reuteri*, a metabolizer of tryptophan, increased the AhR ligands and the capacity of intestinal microbiota to activate AhR, resulting in a reduction of celiac disease [26]. *Lactobacillus* helped restore the AhR activity, improve intestinal permeability, reduce the metabolic syndrome, hepatic steatosis, and *E. coli*-induced mastitis in a mouse model [71, 72]. The administration of immunobiotics increased the genus *Lactobacillus* and *Ruminocccus*, which may increase the production of SCFAs and other metabolites in the MCD group. The protein and mRNA levels of AhR increased in the colonic tissue of the MCD diet-fed mice. The immunobiotic-treated mice had a higher level of AhR-associated genes in both the colonic and liver tissues of mice [21]. The IHC results also confirmed the AhR levels in liver tissues in the immunobiotic-fed mice groups, suggesting that immunobiotics increased the AhR pathway that might help reduce LF. On the other hand, the AhR activation samples were examined *in vitro* using human cell lines. The in vitro study also suggested that fecal samples of mice gavaged with immunobiotics increased the levels of the AhR pathway-associated proteins in both cell lines [15]. Overall, these findings showed that a mixture of immunobiotics helps improve the intestinal barrier integrity, modulate gut microbiota composition, increase the regulatory immune cells and AhR activation in NASH mice, and help ameliorate LF.

Conclusions

This study proposed the possible mechanisms underlying the protective activity of a combination of immunobiotics on the development of NASH and LF progression. Immunobiotics could modulate the gut microbiota composition and increase the SCFA-producing bacteria, and improves the gut barrier strength, resulting in a decrease in serum endotoxin, serum inflammatory cytokine levels, and bacterial translocation. In addition, immunobiotics reduce AhR activation in both colonic and liver tissues, thus reducing liver inflammation and LF progression via the gut–liver axis approach. These findings suggest that immunobiotics have therapeutic potential for preventing NASH and its associated LF.

Declarations

Ethics approval and consent to participate

All experiments involving animals and all study protocols were approved by the animal ethics committee of Dongguk University, South Korea.

Consent for publication

All authors read and approved the manuscript for submission.

Competing interests

The authors declare that there is no conflict of interest

Funding

The authors are grateful for funding support from National Research Foundation (NRF) of Korea grant funded by the Korean Government to Kanmani (NRF-2019R11A1A01058795), and by a grant of the Korea Health Technology R&D Project through the Korea Health Industry Development Institute (KHIDI), funded by the Ministry of Health &Welfare, Republic of Korea (HF20C0020) to Kim as well as by the Korean Research Fellowship (KRF) program of the NRF (2016H1D3A1937971).

Author contributions

PK, JV and HK designed the work and discussed the experiment and results. SKL performed experiments. YDN and EJS were involved in microbial analysis. PK and HK performed the assays. PK and JV wrote the manuscript.

Data availability statement

The data that supports the findings of this study are available as supplementary material in this article. The data are also available from the corresponding author upon reasonable request.

Author details

[1]Department of Rehabilitation medicine of Korean Medicine, Dongguk University, Goyang, Republic of Korea

[2]Department of Anesthesiology, University of Illinois, Chicago, Illinois, USA

[3]Laboratory of Immunobiotechnology, Reference Centre for Lactobacilli (CERELA-CONICET), Tucuman, Argentina

[4]Research Group of Gut Microbiome, Korea Food Research Institute, Wanju-gun 245, Republic of Korea

[5]Department of Food Biotechnology, Korea University of Science and Technology, Wanju, Republic of Korea

References

1. Younossi ZM, Marchesini G, Pinto-Cortez H, Petta S. Epidemiology of Nonalcoholic Fatty Liver Disease and Nonalcoholic Steatohepatitis: Implications for Liver Transplantation. Transplantation. 2019;103(1):22–27.
2. Ferolla SM, Armiliato GN, Couto CA, Ferrari TC. Probiotics as a complementary therapeutic approach in nonalcoholic fatty liver disease. World J Hepatol. 2015;7(3):559–565.
3. Seki E, Schwabe RF. Hepatic inflammation and fibrosis: functional links and key pathways. Hepatol. 2015;61:1066–1079.
4. Yanguas SC, Cogliati B, Willebrords J, Maes M, Colle I, van den Bossche B, et al. Experimental models of liver fibrosis. Arch Toxicol. 2016;90(5):1025–1048.
5. Seki E, De Minicis S, Osterreicher CH, Kluwe J, Osawa Y, Brenner DA, et al. TLR4 enhances TGF-beta signaling and hepatic fibrosis. Nat Med. 2007;13(11):1324–1332.
6. Csak T, Velayudham A, Hritz I, Petrasek J, Levin I, Lippai D, et al. Deficiency in myeloid differentiation factor-2 and toll-like receptor 4 expression attenuates nonalcoholic steatohepatitis and fibrosis in mice. Am J Physiol Gastrointest Liver Physiol. 2011;300(3):G433-G441.
7. Littman DR, Rudensky AY. Th17 and regulatory T cells in mediating and restraining inflammation. Cell. 2010;140:845–858.
8. Xu R, Zhang Z, Wang FS. Liver fibrosis: mechanisms of immune-mediated liver injury. Cell Mol Immunol. 2012;9:296–301.
9. Liu Y, She W, Wang F, et al. 3, 3'-Diindolylmethane alleviates steatosis and the progression of NASH partly through shifting the imbalance of Treg/Th17 cells to Treg dominance. Int Immunopharmacol. 2014;23(2):489–498.
10. Rau M, Schilling AK, Meertens J, Hering I, Weiss J, Jurowich C, et al. Progression from Nonalcoholic Fatty Liver to Nonalcoholic Steatohepatitis Is Marked by a Higher Frequency of Th17 Cells in the Liver and an Increased Th17/Resting Regulatory T Cell Ratio in Peripheral Blood and in the Liver. J Immunol. 2016;196(1):97–105.
11. Tang Y, Bian Z, Zhao L, Liu Y, Liang S, Wang Q, et al. Interleukin-17 exacerbates hepatic steatosis and inflammation in non-alcoholic fatty liver disease. Clin Exp Immunol. 2011;166(2):281–290.
12. Harley IT, Stankiewicz TE, Giles, DA, Softic S, Flick LM, Cappelletti, M et al. IL-17 signaling accelerates the progression of nonalcoholic fatty liver disease in mice. Hepatol. 2014;59:1830–1839.
13. Postler TS, Ghosh S. Understanding the Holobiont: How Microbial Metabolites Affect Human Health and Shape the Immune System. Cell metabolism. 2017;26:110–130,

14. Ivanov II, Frutos RL, Manel N., Yoshinaga K, Rifkin RB, Balfour Sartor R, et al. Specific microbiota direct the differentiation of IL-17-producing T-helper cells in the mucosa of the small intestine. Cell Host Microbe. 2008;4(4):337–349.
15. Marinelli L, Martin-Gallausiaux C, Bourhis JM, Béguet-Crespel F, Blottière HM, Lapaque N. Identification of the novel role of butyrate as AhR ligand in human intestinal epithelial cells. Sci Rep. 2019;9(1):643.
16. Postal BG, Ghezzal S, Aguanno D, André S, Garbin K, Genser L, et al. AhR activation defends gut barrier integrity against damage occurring in obesity. Mol Metab. 2020;39:101007.
17. Lamas B, Natividad JM, Sokol, H. Aryl hydrocarbon receptor and intestinal immunity. Mucosal Immunol. 2018;11:1024–1038.
18. Xiong L, Dean JW, Fu Z, Oliff KN, Bostick JW, Ye J, et al. Ahr-Foxp3-RORgammat axis controls gut homing of CD4(+) T cells by regulating GPR15. Sci Immunol. 2020;5(48):eaaz7277.
19. Furumatsu K, Nishiumi S, Kawano Y, Ooi M, Yoshie T, Shiomi Y, et al. A role of the aryl hydrocarbon receptor in attenuation of colitis. Dig Dis Sci. 2011;56:2532–2544.
20. Duval C, Teixeira-Clerc F, Leblanc AF, Touch S, Emond C, Guerre-Millo M, et al. Chronic exposure to low doses of dioxin promotes liver fibrosis development in the C57BL/6J diet-induced obesity mouse model. Environ Health Perspect. 2017;125:428–436.
21. Yan J, Tung HC, Li S, Niu Y, Garbacz WG, Lu P, et al. Aryl Hydrocarbon Receptor Signaling Prevents Activation of Hepatic Stellate Cells and Liver Fibrogenesis in Mice. Gastroenterol. 2019;157(3):793–806.e14.
22. Ewaschuk, J, Endersby, R, Thiel, D, Diaz, H, Backer J, Ma, M, et al. Probiotic bacteria prevent hepatic damage and maintain colonic barrier function in a mouse model of sepsis. Hepatol 2007; 46:841–850.
23. Li J, Sung CY, Lee N, Ni Y, Pihlajamäki J, Panagiotou G, et al. Probiotics modulated gut microbiota suppresses hepatocellular carcinoma growth in mice. Proc Natl Acad Sci U S A. 2016;113(9):E1306-15.
24. Kanmani P, Suganya K, Kim H. The Gut Microbiota: How Does It Influence the Development and Progression of Liver Diseases. Biomedicines. 2020;8(11):501.
25. Lamas B, Richard ML, Leducq V, et al. CARD9 impacts colitis by altering gut microbiota metabolism of tryptophan into aryl hydrocarbon receptor ligands. Nat. Med. 2016;22:598–605.
26. Lamas B, Hernandez-Galan L, Galipeau HJ, Constante M, Clarizio A, Jury J, et al. Aryl hydrocarbon receptor ligand production by the gut microbiota is decreased in celiac disease leading to intestinal inflammation. Sci Transl Med. 2020;12(566):eaba0624.
27. Kanmani P, Kim H. Protective Effects of Lactic Acid Bacteria Against TLR4 Induced Inflammatory Response in Hepatoma HepG2 Cells Through Modulation of Toll-Like Receptor Negative Regulators of Mitogen-Activated Protein Kinase and NF-kB signaling. Front Immunol. 2018;9:1537.
28. Kanmani, P, Kim, H. Immunobiotic Strains Modulate Toll-Like Receptor 3 Agonist Induced Innate Antiviral Immune Response in Human Intestinal Epithelial Cells by Modulating IFN Regulatory Factor

3 and NF-κB Signaling. Front. Immunol. 2019;10:1536.

29. Caporaso JG, Kuczynski J, Stombaugh J, Bittinger K, Bushman FD, Costello EK, et al. QIIME allows analysis of high-throughput community sequencing data. Nat. Methods. 2010;7:335–336.
30. Segata N, Izard J, Waldron L, Gevers D, Miropolsky L, Garrett WS, et al. Metagenomic biomarker discovery and explanation. Genome Biol. 2011;12(6):R60.
31. Hebbard L, George J. Animal models of nonalcoholic fatty liver disease. Nat. Rev. Gastroenterol. Hepatol. 2011;8:35–44.
32. Rolla S, Alchera E, Imarisio C, Bardina V, Valente G, Cappello P, et al. The balance between IL-17 and IL-22 produced by liver-infiltrating T-helper cells critically controls NASH development in mice. Clin Sci. (Lond). 2016;130(3):193–203.
33. Machado MV, Michelotti GA, Xie G, de Almeida TP, Boursier J, Bohnic B, et al. Mouse Models of Diet-Induced Nonalcoholic Steatohepatitis Reproduce the Heterogeneity of the Human Disease. PLoS ONE. 2015;10(5): e0127991.
34. Wigg AJ, Roberts-Thomson IC, Dymock RB, McCarthy PJ, Grose RH, Cummins AG. The role of small intestinal bacterial overgrowth, intestinal permeability, endotoxaemia, and tumour necrosis factor alpha in the pathogenesis of non-alcoholic steatohepatitis. Gut. 2001;48:206–211.
35. Luther J, Garber, JJ, Khalili H, Dave M, Bale SS, Jindal R, et al. Hepatic injury in nonalcoholic steatohepatitis contributes to altered intestinal permeability. Cell Mol. Gastroenterol. Hepatol. 2015;1:222–232.
36. Yu T, Chen X, Zhang W, Li L, Xu R, Wang TC, et al. Kru¨ppel-like Factor 4 Regulates Intestinal Epithelial Cell Morphology and Polarity. PLoS ONE. 2012;7(2):e32492.
37. Endo H, Niioka M, Kobayashi N, Tanaka M, Watanabe T. Butyrate-Producing Probiotics Reduce Nonalcoholic Fatty Liver Disease Progression in Rats: New Insight into the Probiotics for the Gut-Liver Axis. PLoS ONE. 2013;8(5): e63388.
38. Jiang W, Wu N, Wang X, Chi Y, Zhang Y, Qiu X, et al. Dysbiosis gut microbiota associated with inflammation and impaired mucosal immune function in intestine of humans with non-alcoholic fatty liver disease. Sci Rep. 2015;5:8096.
39. Boursier J, Mueller O, Barret M, Machado M, Fizanne L, Araujo-Perez F, et al. The severity of nonalcoholic fatty liver disease is associated with gut dysbiosis and shift in the metabolic function of the gut microbiota. Hepatol. 2016;63(3):764–775.
40. Velázquez KT, Enos RT, Bader JE, Sougiannis AT, Carson MS, Chatzistamou I, et al. Prolonged high-fat-diet feeding promotes non-alcoholic fatty liver disease and alters gut microbiota in mice. World J Hepatol. 2019; 11(8):619–637.
41. Xie X, Zhang L, Yuan S, Li H, Zheng C, Xie S, et al. Val-Val-Tyr-Pro protects against non-alcoholic steatohepatitis in mice by modulating the gut microbiota and gut-liver axis activation. J Cell Mol Med. 2021;25(3):1439–1455.
42. Lee G, You HJ, Bajaj JS, Joo SK, Yu J, Park S, et al. Distinct signatures of gut microbiome and metabolites associated with significant fibrosis in non-obese NAFLD. Nat Commun. 2020;11(1):4982.

43. Kawauchi S, Horibe S, Sasaki N, Tanahashi T, Mizuno S, Hamaguchi T, Rikitake Y. Inhibitory Effects of Sodium Alginate on Hepatic Steatosis in Mice Induced by a Methionine- and Choline-deficient Diet. Mar Drugs. 2019;17(2):104.
44. Brawner KM, Yeramilli VA, Duck LW, Van Der Pol W, Smythies LE, Morrow CD, et al. Depletion of dietary aryl hydrocarbon receptor ligands alters microbiota composition and function. Sci Rep. 2019;9(1):14724.
45. Velayudham A, Dolganiuc A, Ellis M, Petrasek J, Kodys K, et al. VSL#3 probiotic treatment attenuates fibrosis without changes in steatohepatitis in a diet-induced nonalcoholic steatohepatitis model in mice. Hepatol. 2009;49:989–997.
46. Ye J, Lv L, Wu W, Li Y, Shi D, Fang D, et al. Butyrate Protects Mice Against Methionine–Choline-Deficient Diet-Induced Non-alcoholic Steatohepatitis by Improving Gut Barrier Function, Attenuating Inflammation and Reducing Endotoxin Levels. Front. Microbiol. 2018;9:1967.
47. Cani PD, Amar J, Iglesias MA, Poggi M, Knauf C, Bastelica D, et al. Metabolic endotoxemia initiates obesity and insulin resistance. Diabetes. 2007;56(7):1761–1772.
48. Kessoku T, Kobayashi T, Imajo K, Tanaka K, Yamamoto A, Takahashi K, et al. Endotoxins and Non-Alcoholic Fatty Liver Disease. Front. Endocrinol. 2021;12:770986.
49. Giorgio V, Miele L, Principessa L, Ferretti F, Villa MP, Negro V, et al. Intestinal permeability is increased in children with non-alcoholic fatty liver disease, and correlates with liver disease severity. Dig Liver Dis. 2014;46(6):556–60.
50. Ritze Y, Bárdos G, Claus A, Ehrmann V, Bergheim I, Schwiertz A, et al. *Lactobacillus rhamnosus* GG protects against non-alcoholic fatty liver disease in mice. PLoS ONE. 2014; 9(1):e80169.
51. Matthews DR, Li H, Zhou J, Li Q, Glaser S, Francis H, et al. Methionine- and Choline-Deficient Diet-Induced Nonalcoholic Steatohepatitis Is Associated with Increased Intestinal Inflammation. Am J Pathol. 2021;191(10):1743–1753.
52. Xue L, He J, Gao N, Lu X, Li M, Wu X, et al. Probiotics may delay the progression of nonalcoholic fatty liver disease by restoring the gut microbiota structure and improving intestinal endotoxemia. Sci Rep. 2017;7:45176.
53. Xiong F, Zheng Z, Xiao L, Su C, Chen J, Gu X, et al. Soyasaponin A2 Alleviates Steatohepatitis Possibly through Regulating Bile Acids and Gut Microbiota in the Methionine and Choline-Deficient (MCD) Diet-induced Nonalcoholic Steatohepatitis (NASH) Mice. Mol Nutr Food Res. 2021;65(14):e2100067.
54. Wang Y, Zhang Y, Yang J, Li, H.; Wang J, Geng W. *Lactobacillus plantarum* MA2 Ameliorates Methionine and Choline-Deficient Diet Induced Non-Alcoholic Fatty Liver Disease in Rats by Improving the Intestinal Microecology and Mucosal Barrier. Foods. 2021;10:3126.
55. Yu JS, Youn GS, Choi J, Kim CH, Kim BY, Yang SJ, et al. *Lactobacillus lactis* and *Pediococcus pentosaceus*-driven reprogramming of gut microbiome and metabolome ameliorates the progression of non-alcoholic fatty liver disease. Clin Transl Med. 2021;11(12):e634.

56. Guo J, Friedman SL. Toll-like receptor 4 signaling in liver injury and hepatic fibrogenesis. Fibrogenesis Tissue Rep. 2010;3:21.
57. Zhu Q, Zou L, Jagavelu K, Simonetto DA, Huebert RC, Jiang ZD, et al. Intestinal decontamination inhibits TLR4 dependent fibronectin mediated crosstalk between stellate cells and endothelial cells in liver fibrosis in mice. J. Hepatol. 2012;56:893–899.
58. Cai C, Zhu X, Li P, Li J, Gong J, Shen W, et al. (2017). NLRP3 deletion inhibits the non-alcoholic steatohepatitis development and inflammation in Kupper cells induced by palmitic acid. Inflammation. 2017;40:1875–1883.
59. Yang L, Seki E. Toll- like receptors in liver fibrosis: cellular crosstalk and mechanisms. Front. Physio. 2012;3:138.
60. Taniki N, Nakamoto N, Chu PS, Ichikawa M, Teratani T, Kanai T. Th17 cells in the liver: balancing autoimmunity and pathogen defense. Semin Immunopathol. 2022.
61. Fabre T, Kared H, Friedman SL, Shoukry NH. IL-17A enhances the expression of profibrotic genes through upregulation of the TGF-b receptor on hepatic stellate cells in a JNK-dependent manner. J Immunol. 2014;193:3925–3933.
62. Meng F, Wang K, Aoyama T, Grivennikov SI, Paik Y, Scholten D, et al. Interleukin-17 signaling in inflammatory, Kupffer cells, and hepatic stellate cells exacerbates liver fibrosis in mice. Gastroenterol. 2012;143:765–776.
63. Verma R, Lee C, Jeun EJ, Yi J, Kim KS, Ghosh A, et al. Cell surface polysaccharides of *Bifidobacterium bifidum* induce the generation of Foxp3 (+) regulatory T cells. Sci Immunol. 2018;3:eaat6975.
64. Xu R, Tao A, Zhang S, Zhang M. Neutralization of interleukin-17 attenuates high fat diet-induced non-alcoholic fatty liver disease in mice. Acta Biochim Biophys Sin. 2013;45:726–733.
65. Hartmann P, Duan Y, Miyamoto Y, Demir M, Lang S, Hasa E, et al. Colesevelam ameliorates non-alcoholic steatohepatitis and obesity in mice. Hepatol Int. 2022.
66. Zhang X, Coker OO, Chu ES, Fu K, Lau HCH, Wang YX, et al. Dietary cholesterol drives fatty liver-associated liver cancer by modulating gut microbiota and metabolites. Gut. 2021;70(4):761–774.
67. Zhang H, Liu M, Liu X, Zhong W, Li Y, Ran Y, et al. *Bifidobacterium animalis* ssp. *Lactis* 420 Mitigates Autoimmune Hepatitis Through Regulating Intestinal Barrier and Liver Immune Cells. Front. Immunol. 2020;11:569104.
68. Schwiertz A, Taras D, Schäfer K, Beijer S, Bos NA, Donus C, et al. Microbiota and SCFA in lean and overweight healthy subjects. Obesity. (Silver Spring). 2010;18(1):190–195.
69. Eslamparast T, Eghtesad S, Hekmatdoost A, Poustchi H. Probiotics and nonalcoholic fatty liver disease. Middle East J Dig Dis. 2013;5(3):129–136.
70. Loomba R, Seguritan V, Li W, Long T, Klitgor N, Bhatt A, et al. Gut microbiome-based metagenomic signature for non-invasive detection of advanced fibrosis in human nonalcoholic fatty liver disease. Cell Metab. 2019;25;1054–1062.

71. Natividad JM, Agus A, Planchais, J, Lamas B, Jarry AC, Martin R, et al. Impaired aryl hydrocarbon receptor ligand production by the gut Microbiota is a key factor in metabolic syndrome. Cell Metab. 2018;28: 737–749.
72. Zhao C, Hu X, Bao L, Wu K, Feng L, Qiu M, et al. Aryl hydrocarbon receptor activation by *Lactobacillus reuteri* tryptophan metabolism alleviates *Escherichia coli*-induced mastitis in mice. PLoS Pathog. 2021;17(7):e1009774.

Figures

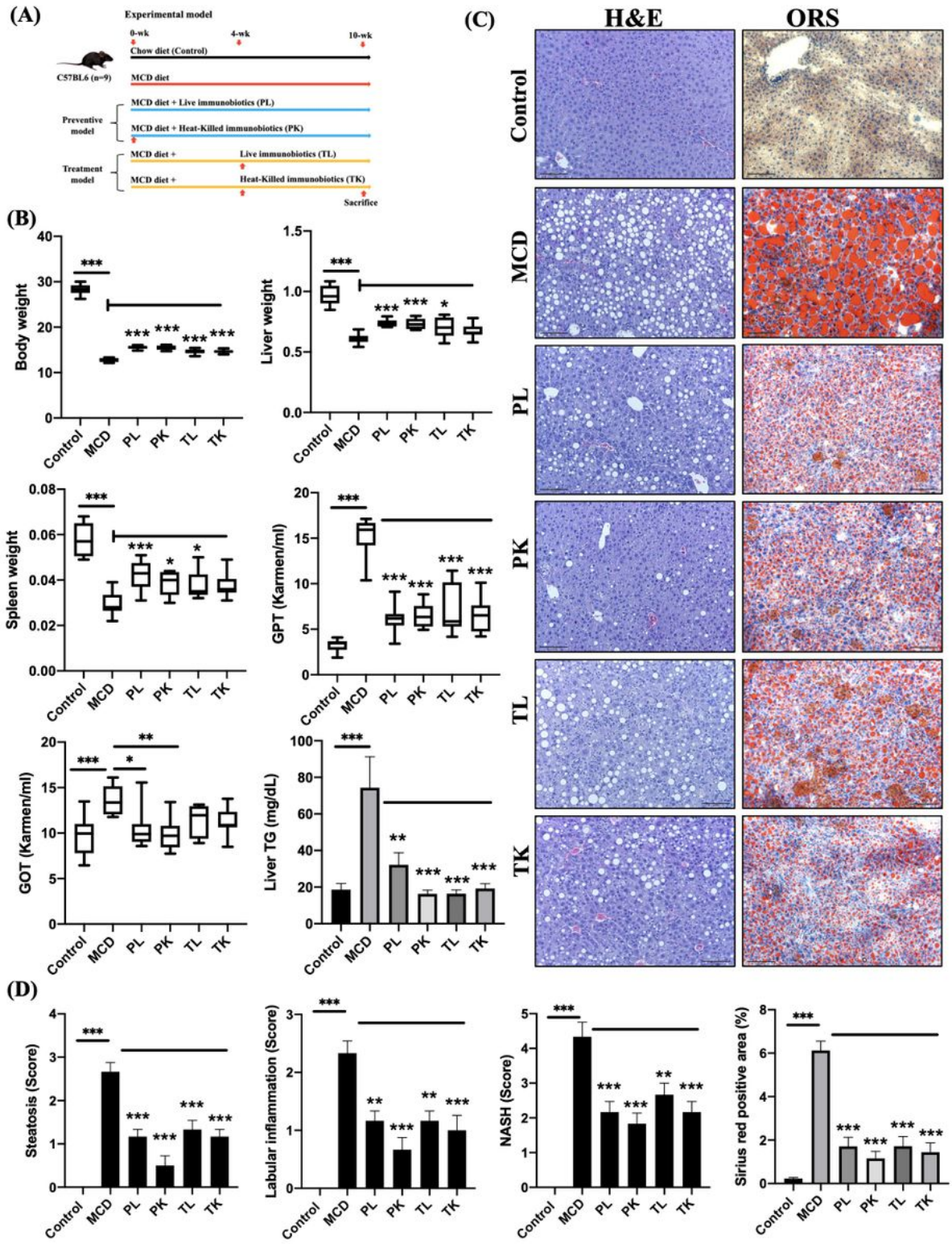

Figure 1

Immunobiotics administration attenuated MCD diet-induced hepatic inflammation in mice. Mice were fed with MCD diet or chew diet for 10 weeks; immunobiotics mixture (live and heat-killed) were administrated for the 10 weeks or for the last 6 weeks of MCD diet. (A) Experimental model of LF and immunobiotics treatment. (B) Body, liver and spleen weights and serum concentration of GPT and GOT, and Liver TG of

each group of mice (n=9). (C &D) Representative liver histology pictures and scores of each group mice (n=6). The data were presented as means ± SD. * p< 0.05, **p<0.01, ***p<0.001.

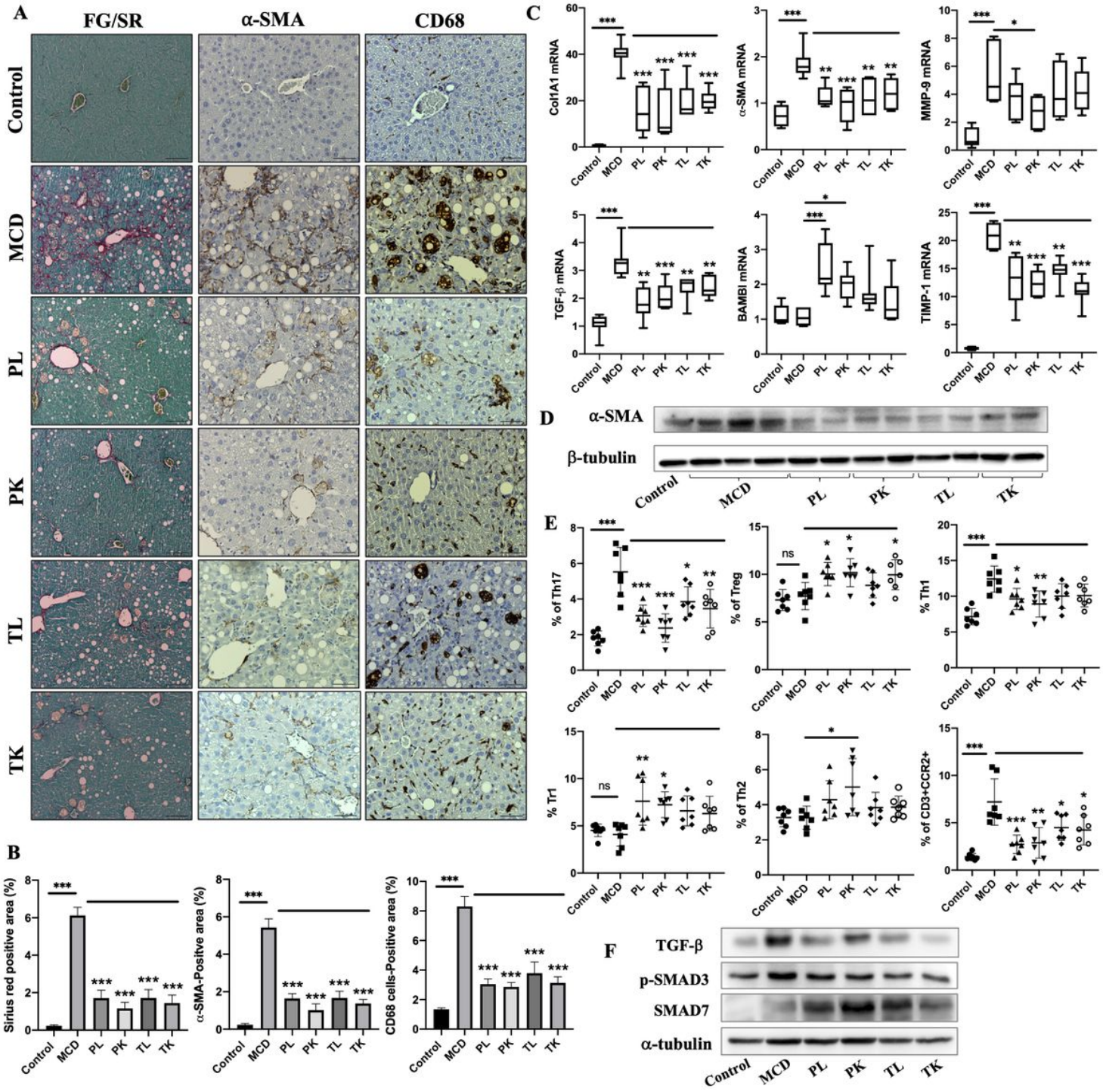

Figure 2

Immunobiotics reduced MCD diet-induced LF in mice. (A) Liver sections were analyzed for collagen deposition using Fastgreen/Sirius Red staining and for a-SMA and CD68 using immune-histochemistry. (B) The contents of collagen, a-SMA and CD68 were quantified. (C) The expression of profibrogenic markers were determined in the liver tissues using RT-PCR. The data were presented as means ± SD

(n=9). (D) The protein level of a-SMA in the liver tissue was analysed by western blot. (E) The frequency of different subpopulations of T cells in liver tissue of mice with LF (n=6). (F). The protein level of TGF-b signaling associated proteins were analysed in the liver tissue of mice using western blot. * p< 0.05, **p<0.01, ***p<0.001.

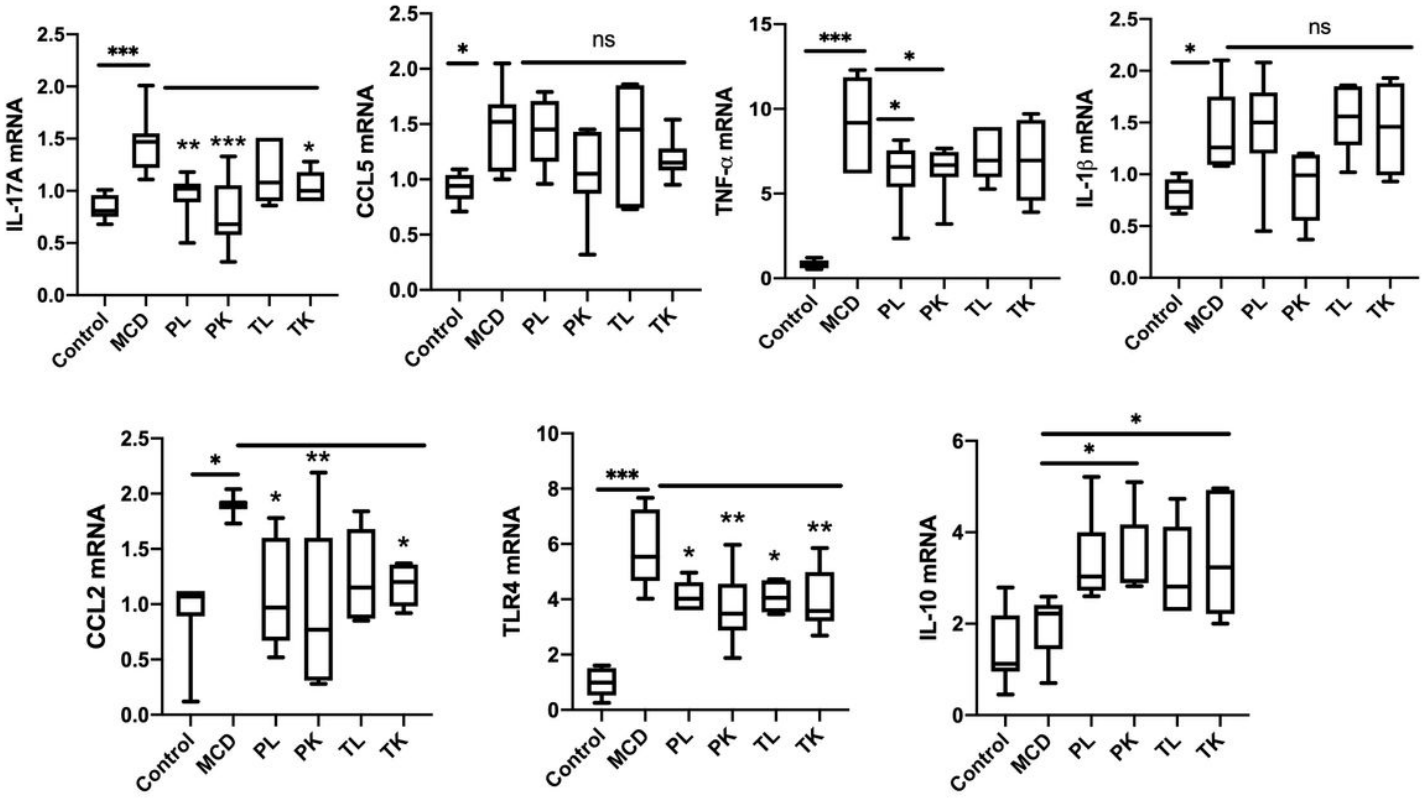

Figure 3

Immunobiotics reduced inflammatory makers in LF mice. The expression of pro-inflammatory cytokines, TLR4 and anti-inflammatory cytokine (IL-10) in the liver tissues of mice with LF. The data were presented as means ± SD (n=9). * p< 0.05, **p<0.01, ***p<0.001.

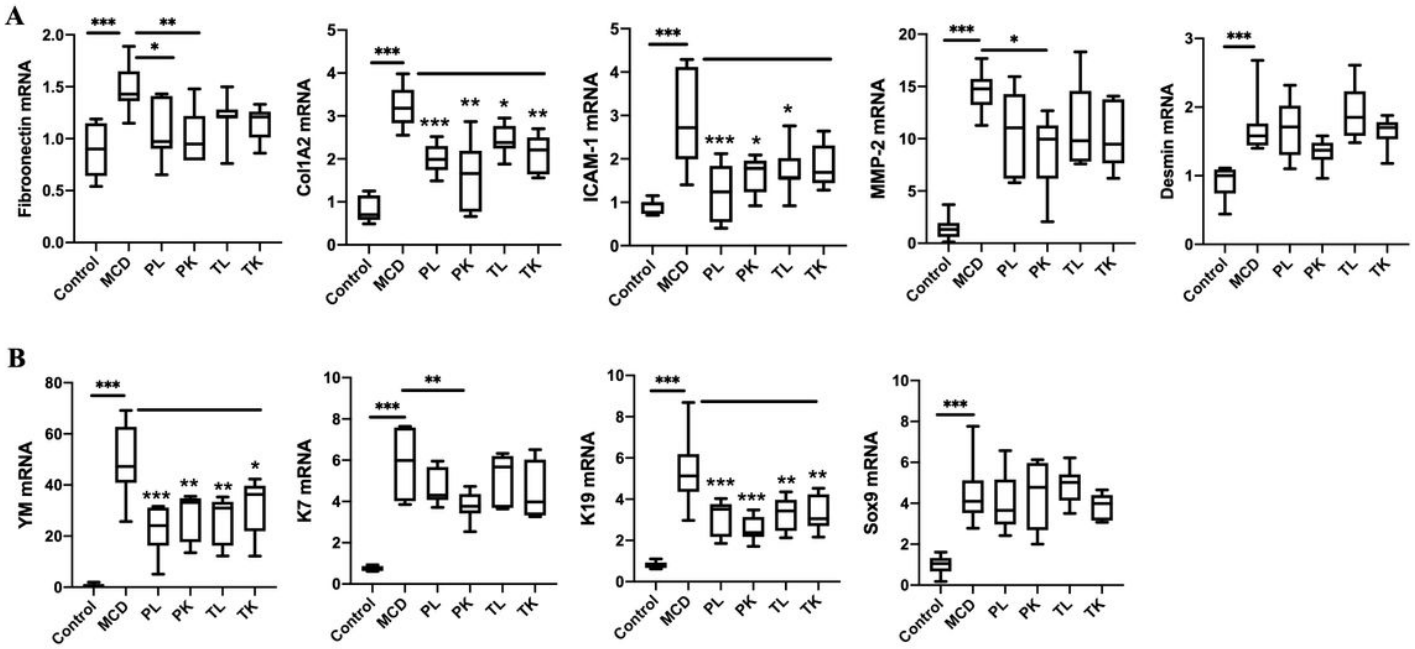

Figure 4

Immunobiotics reduced profibrogenic makers in LF mice. (A) RT-PCR results of liver pro-fibrogenic markers (Fibronectin, Col1A2, ICAM-1, MMP-2 and Desmin) (B) The expression of macrophage and progenitor markers were determined in the liver tissue of mice with LF. The data were presented as means ± SD (n=9). * p< 0.05, **p<0.01, ***p<0.001.

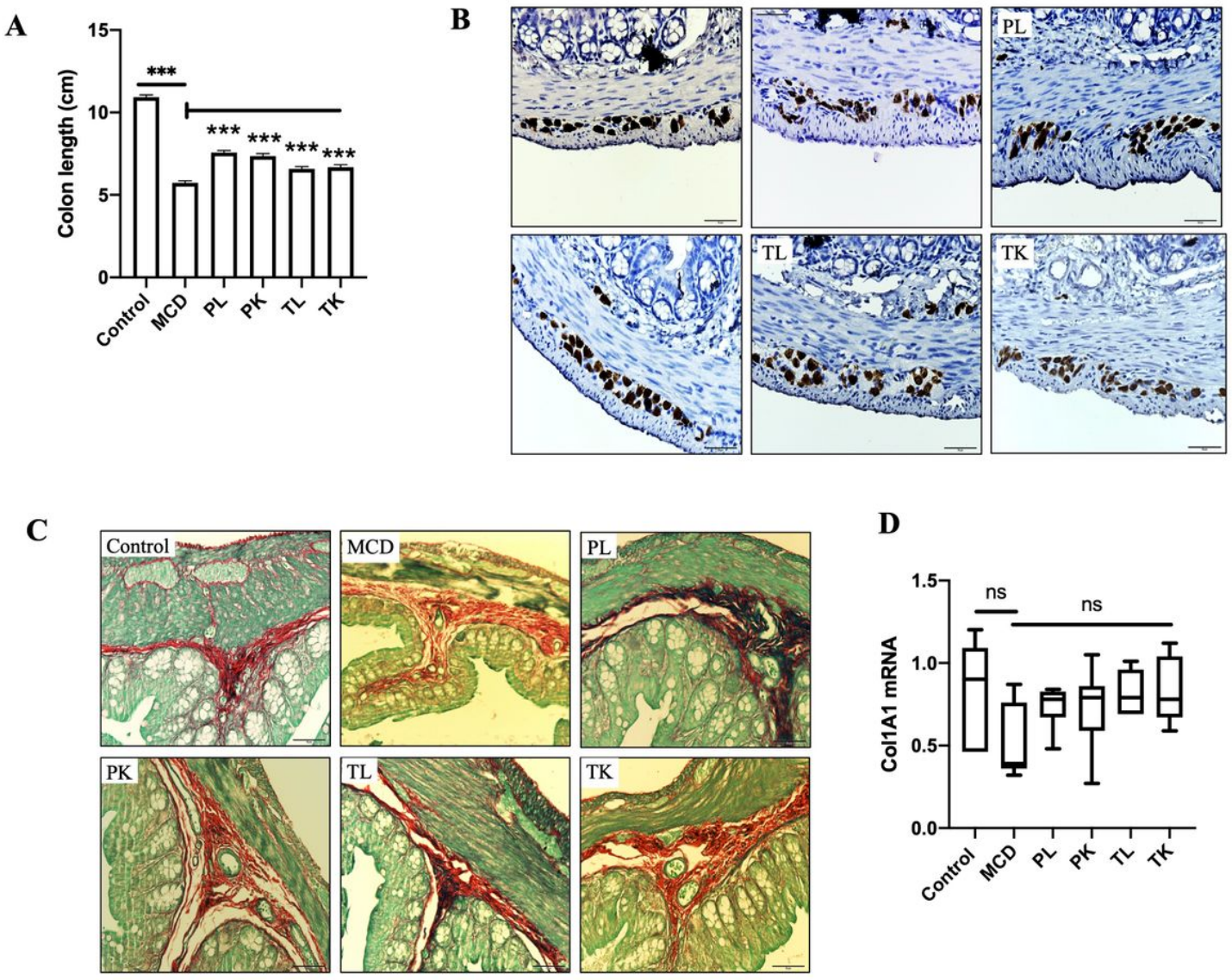

Figure 5

Immunobiotics improved colonic length in LF mice. (A) The colonic length of mice was determined for the 10 weeks of MCD or chew diet along with immunobiotics fed mice. (B) colons were immunostained for the determination of myenteric ganglia with number neurons. (C) Fastgreen/Sirius Red staining were performed the observation of collagen fibres in the colonic tissue of mice. (D) Collagen fibres quantified in the colonic tissue of mice. The data were presented as means ± SD (n=5). ***p<0.001.

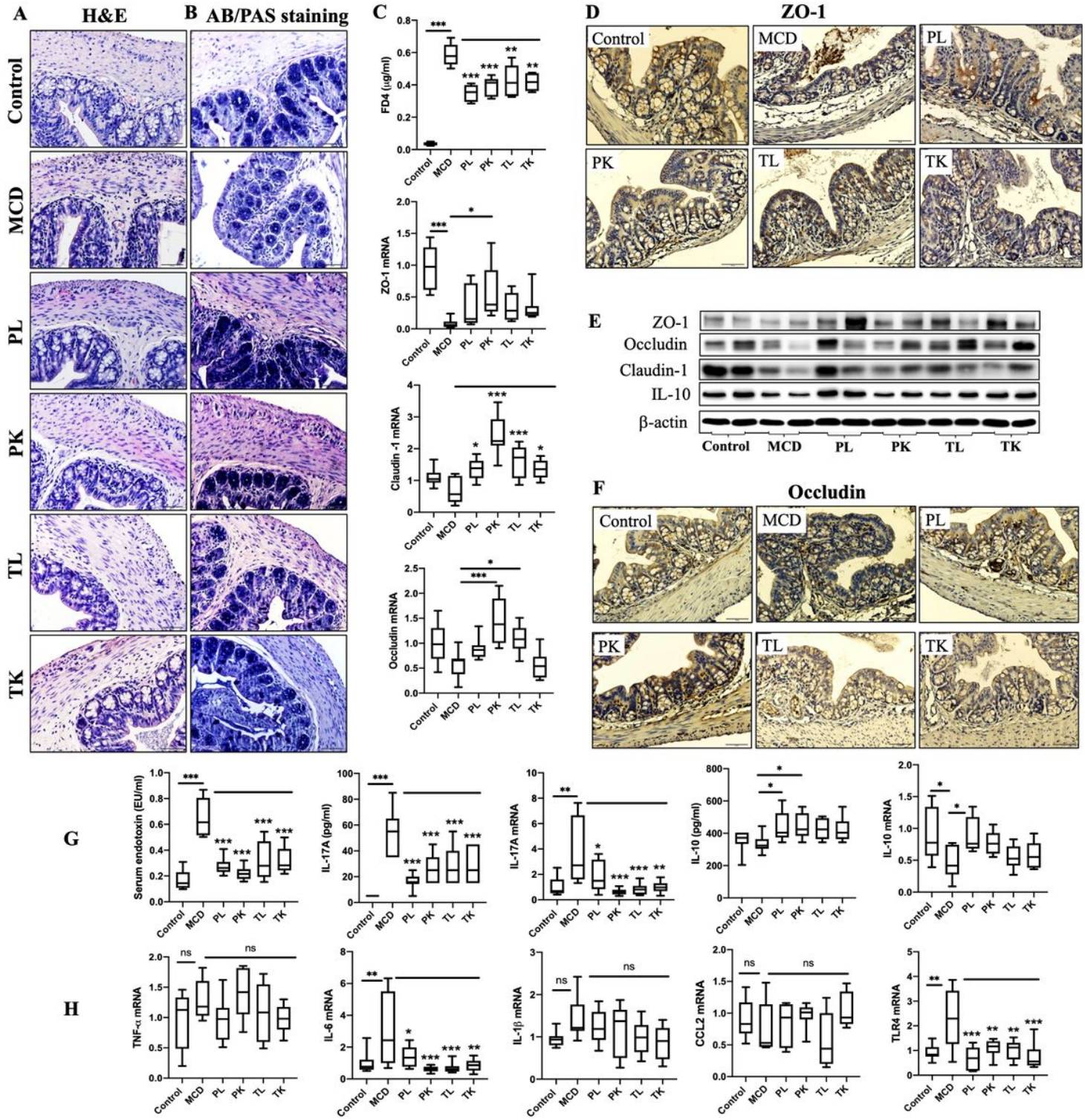

Figure 6

Immunobiotics treatment improved MCD diet induced colonic morphological changes and strength in LF mice. (A) Hematoxylin and eosin (H&E) stained sections of colonic tissue of mice fed with MCD diet or chew diet along with immunobiotics. (B)AB/PAS staining of colonic tissue with goblet cells and mucus. (C) In vivo intestinal permeability was analysed by FD4 and the expression of tight-junction genes in the colonic tissue of mice using RT-PCR. (D) Immunostaining of ZO-1 protein in the colonic tissue. (E) The level of tight-junction proteins (ZO-1, Occludin and Claudin-1) and IL-10 in the colonic tissue were

analysed by WB. (F) Immunostaining of occluding in the colonic tissue. (G) Serum endotoxin level was determined using LAL assay and serum IL-17A and IL-10 and their mRNA levels were analyzed by ELISA and RT-PCR. (H). The expression of pro-inflammatory cytokines and TLR4 were analyzed in the colonic tissue using RT-PCR. The data were presented as means ± SD (n=9). * p< 0.05, **p<0.01, ***p<0.001.

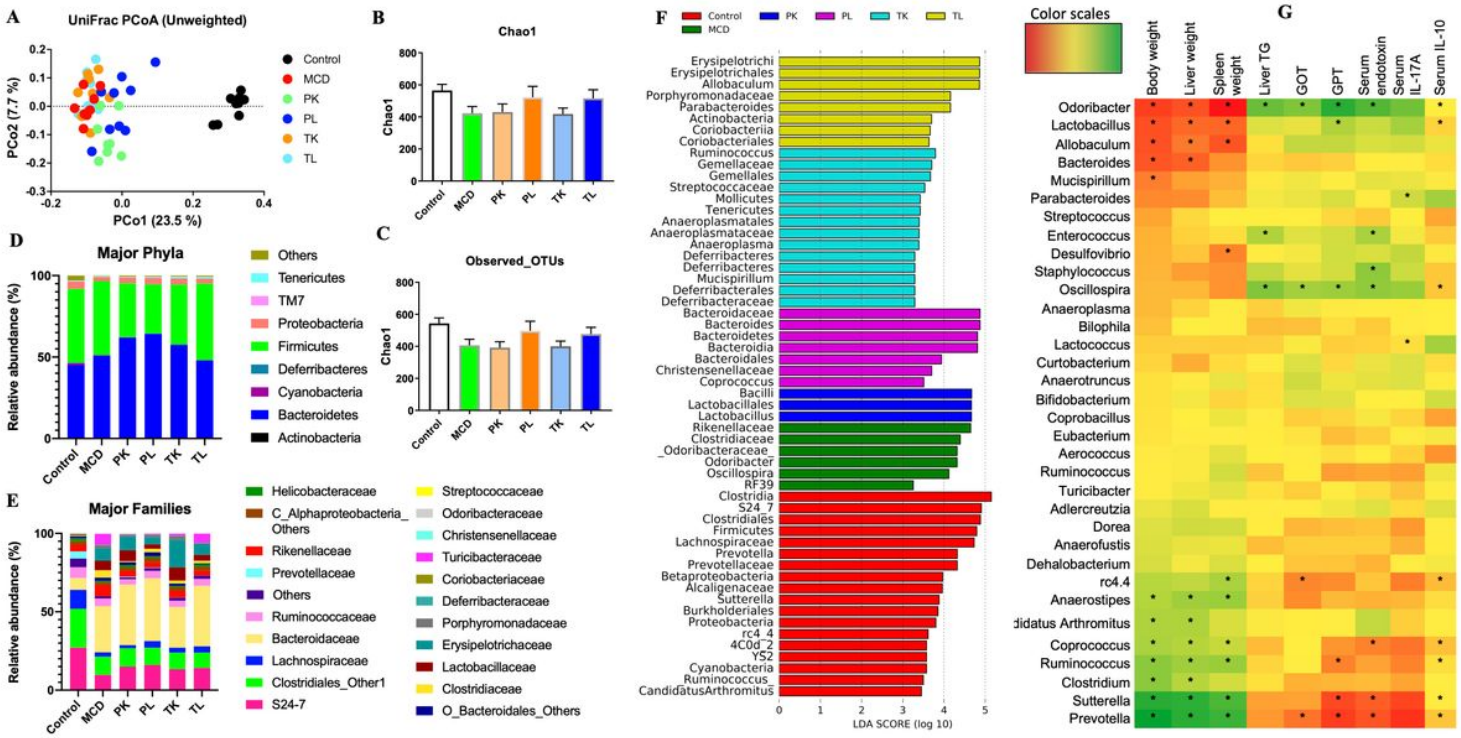

Figure 7

Immunobiotics modulated composition and diversity of gut microbiota in LF mice. The gut microbiota composition was analyzed using total DNA from mice fecal samples that collected at the end of the experiments. (A) Unweighted Unifrac analysis, (B) Chao1, (C) Observed OTUs were showed among the groups. (D and E) Relative abundance of bacterial taxa at the phylum and family levels among the groups. (F) Microbial taxa respond to MCD diet and immunobiotic treatement were examined using LDA effect size assay. (G) The correlation of the gut microbiota with the disease markers were examined using R and R studio programs.

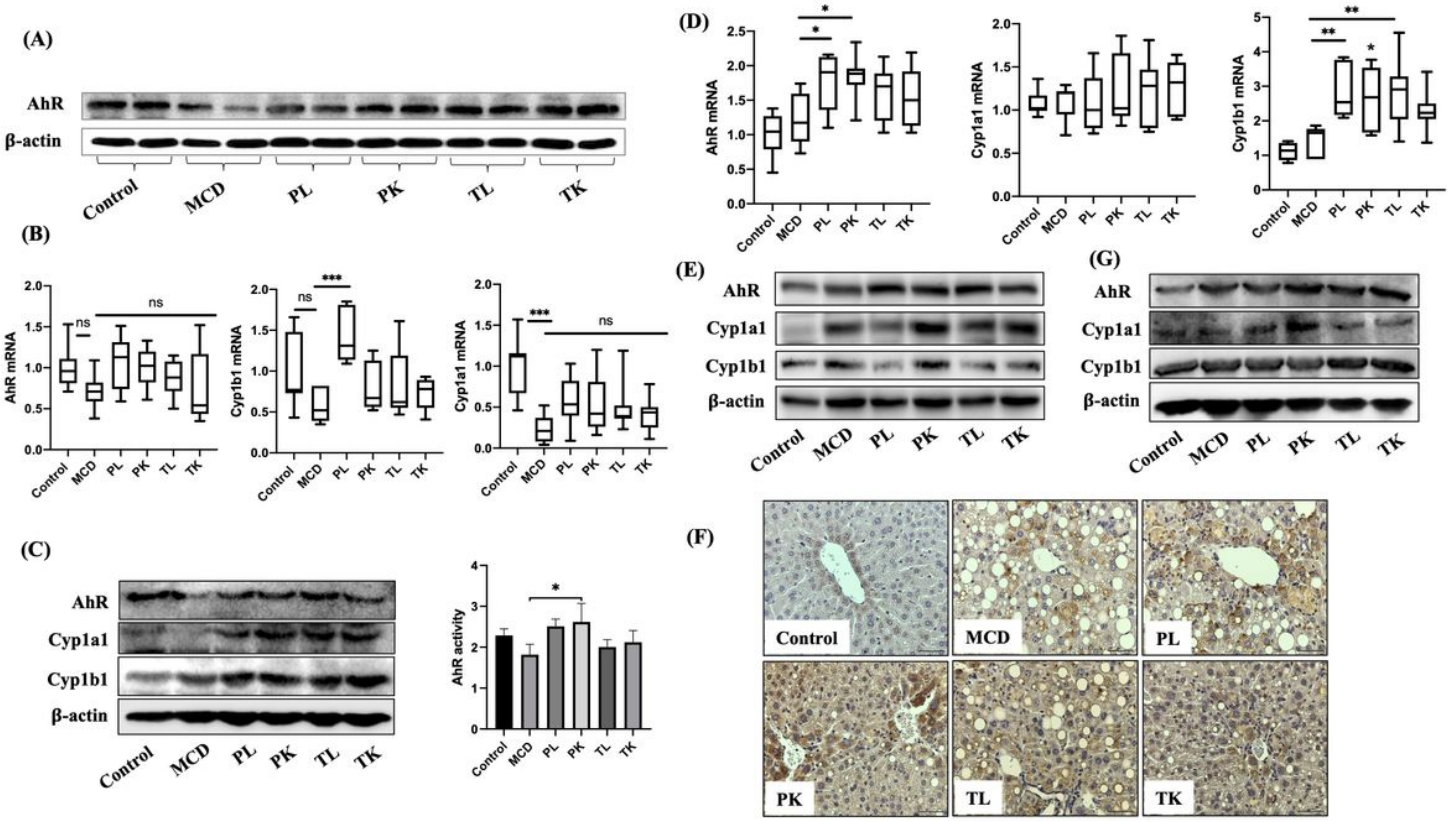

Figure 8

Immunobiotics induced AhR activation in the colonic and liver tissues of mice and LX-2 cells. (A) The protein level of AhR and (B) mRNA levels AhR associated markers were analysed in colonic tissue of mice using WB and RT-PCR. (C) The protein level of AhR and it's associated markers and AhR activity were analyzed in colonic epithelial cells (n=6). (D) The expression of AhR and it's associated markers were analyzed in liver tissues of mice using RT-PCR. (E) The protein level of AhR and it's associated markers were analyzed in liver tissues of mice and (F) LX-2 cells (n=6). (G) Liver tissue was immunostained for the determination of AhR positive cells. The data were presented as means ± SD. * p< 0.05, **p<0.01, ***p<0.001.

Supplementary Files

This is a list of supplementary files associated with this preprint. Click to download.

- SuplFig1.jpg
- SuplFig2.jpg
- SuplFig3.jpg
- SuplFig4.jpg
- SuplTable1.docx